Science Advances

AAAS

advances.sciencemag.org/cgi/content/full/3/9/e1603187/DC1

Supplementary Materials for

Inward H^+ pump xenorhodopsin: Mechanism and alternative optogenetic approach

Vitaly Shevchenko, Thomas Mager, Kirill Kovalev, Vitaly Polovinkin, Alexey Alekseev, Josephine Juettner, Igor Chizhov, Christian Bamann, Charlotte Vavourakis, Rohit Ghai, Ivan Gushchin, Valentin Borshchevskiy, Andrey Rogachev, Igor Melnikov, Alexander Popov, Taras Balandin, Francisco Rodriguez-Valera, Dietmar J. Manstein, Georg Bueldt, Ernst Bamberg, Valentin Gordeliy

Published 22 September 2017, *Sci. Adv.* **3**, e1603187 (2017)
DOI: 10.1126/sciadv.1603187

This PDF file includes:

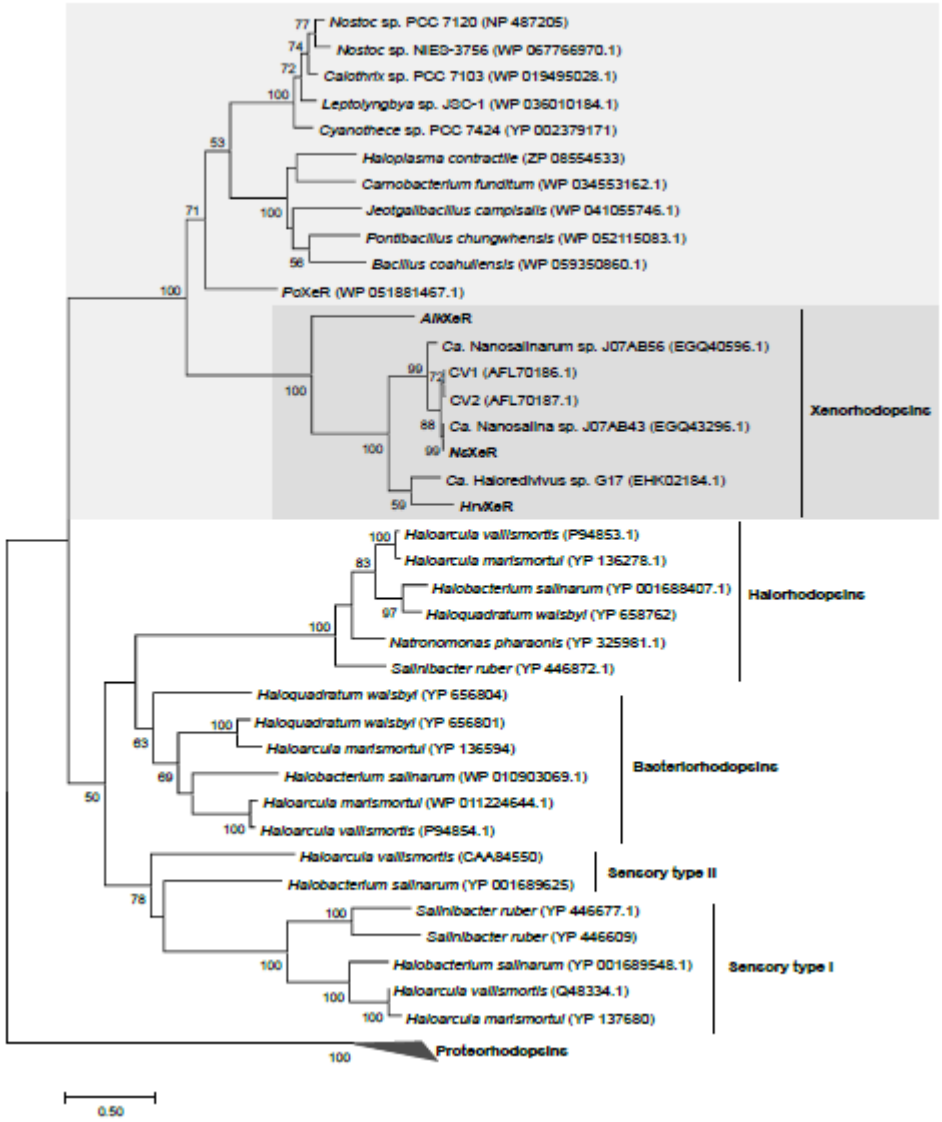

fig. S1. Phylogenetic tree of microbial rhodopsin proteins. 38 rhodopsin sequences were aligned using MUSCLE. Phylogenetic reconstruction was conducted by maximum-likelihood (ML) using MEGA6 with the following parameters: Jones-Taylor-Thornton model, 100 bootstraps, gamma distribution with five discrete categories, positions with less than 80% site coverage were eliminated. Only bootstraps greater than 50% are shown. Genbank accesion numbers are written in parentheses for each protein. The genes, which encode the proteins studied in our work are in bold.

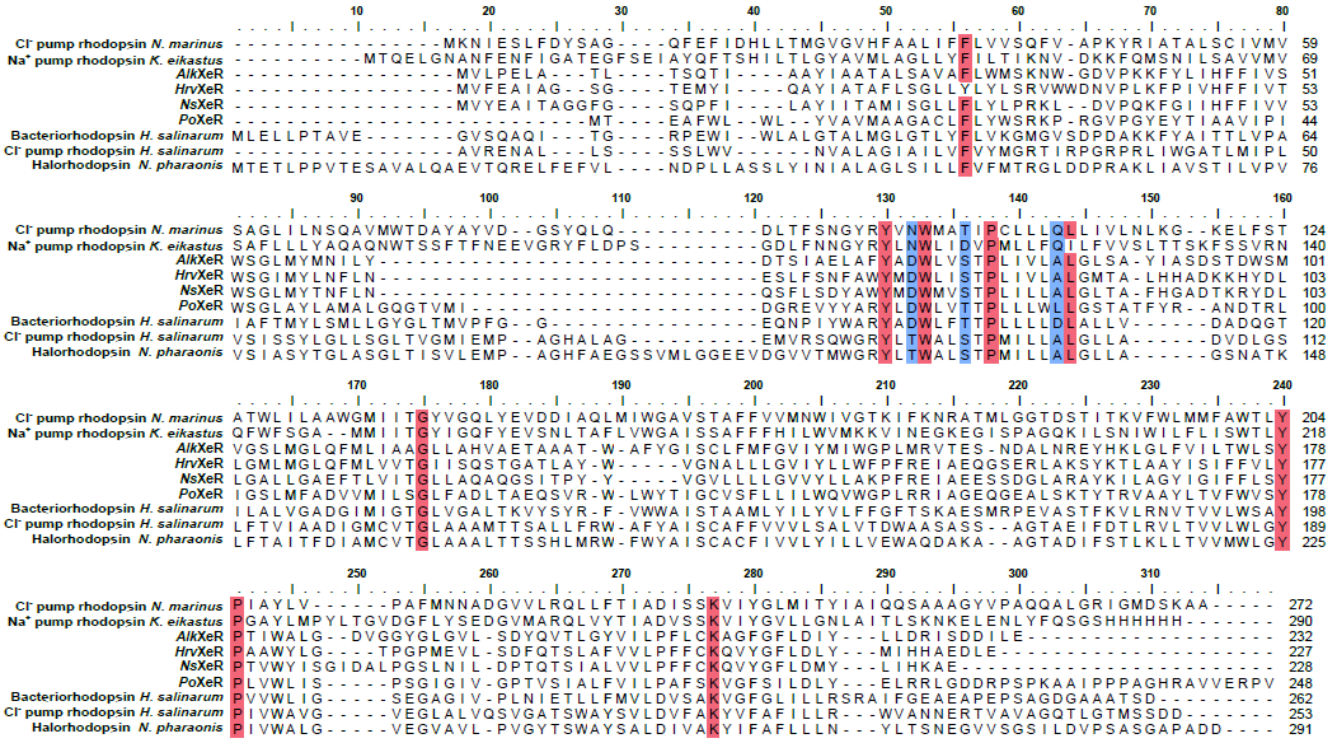

fig. S2. Sequence alignment of microbial rhodopsins. The sequence alignment was performed with Clustal Omega. The motif amino acids are colored blue. Highly conserved regions are colored red.

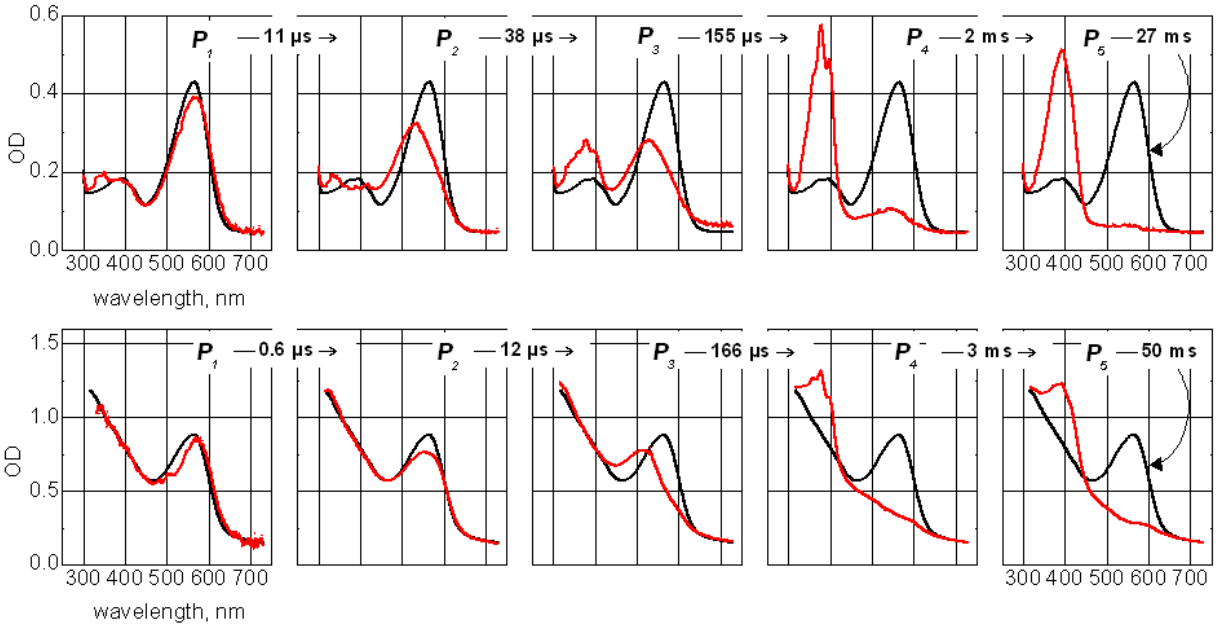

fig. S3. Photocycles of the *Ns*XeR in nanodisc (ND, upper row) and liposome (LIP, lower row) preparations (20°C, pH 7.5). Five kinetically distinct protein states (red lines) are obtained via global multi exponential analysis of the flash photolysis data exemplified in the Fig. 2b. An each panel contains for the reference the correspondent spectrum on unexcited protein (P_0, black lines). The spectra of $P_{i=1..5}$ states were calculated from correspondent spectra of exponents, which were further converted to the differential spectra of the states assuming the sequential irreversible model of the photocycle. The half-times of reactions are depicted between the panels. The fraction of cycled molecules was 12.5 % in ND, and 15 % in LIP.

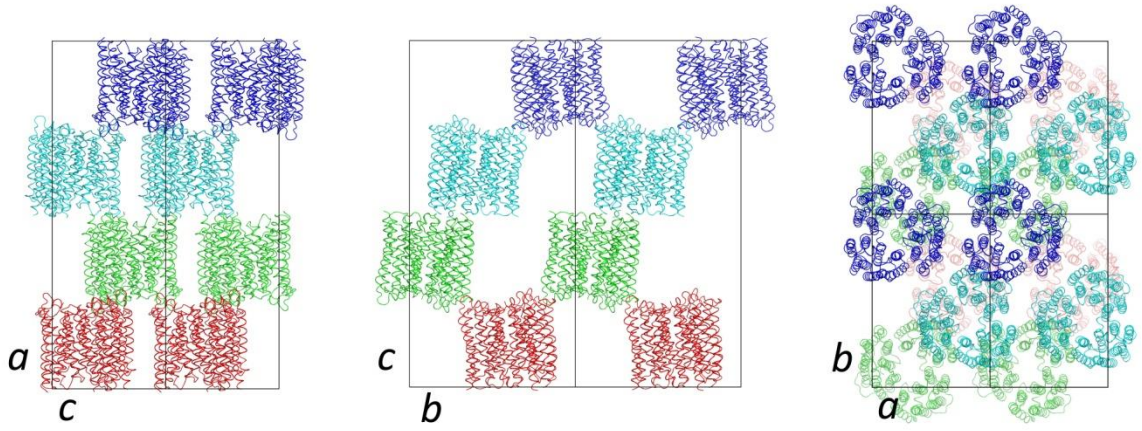

fig. S4. Crystal packing of *Ns*XeR.

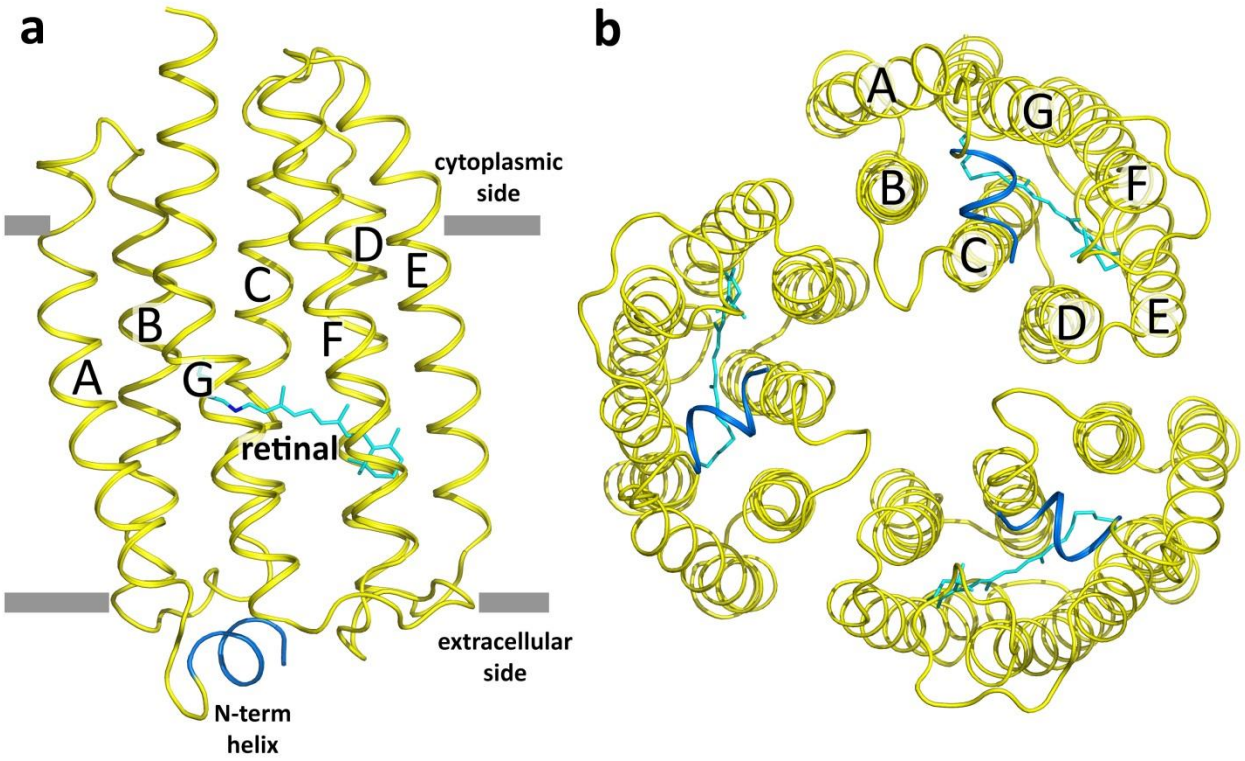

fig. S5. Overall architecture of *Ns*XeR. a. *Ns*XeR fold. **b**. *Ns*XeR trimer. The N-terminal α-helix is colored blue. Helices A-G are subscribed, retinal is colored cyan. The hydrophobic membrane core boundaries were calculated using the PPM server and are shown by the gray lines.

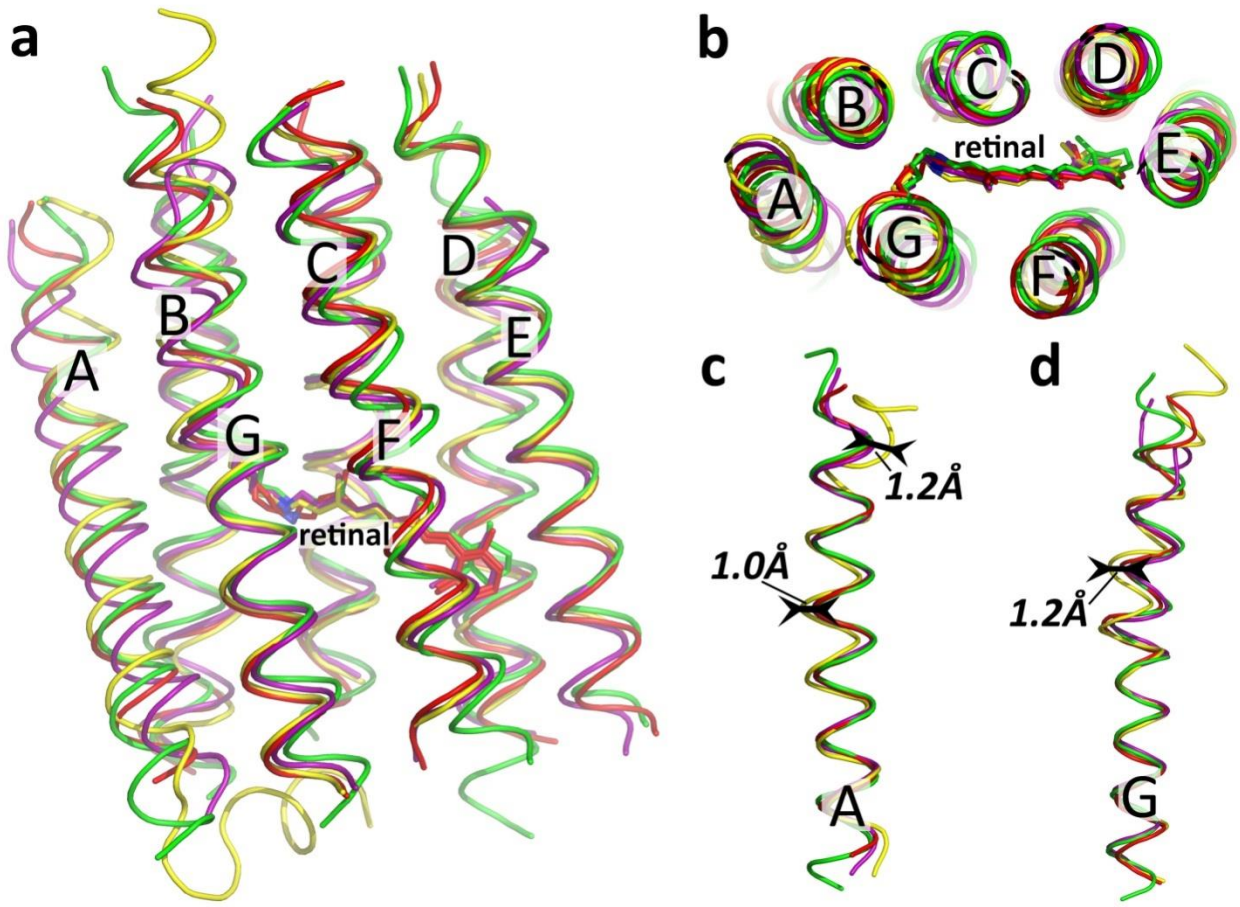

fig. S6. Comparison of *Ns*XeR structure with structures of other microbial rhodopsins.
a. Comparison of the *Ns*XeR backbone structure with those of bacteriorhodopsin (BR, purple, PDB 1C3W), anabaena sensory rhodopsin (ASR, red, PDB 1XIO) and proteorhodopsin (ESR, green, PDB 4HYJ). The loops and termini (except N-terminal helix of *Ns*XeR) are not shown. **b**. Comparison of the retinal positions from the cytoplasmic side of the protein. **c**. Comparison of helix A separately. The deviations of *Ns*XeR helix A are shown with arrows. **d**. Comparison of helix G separately. The deviations of *Ns*XeR helix G are shown with arrows.

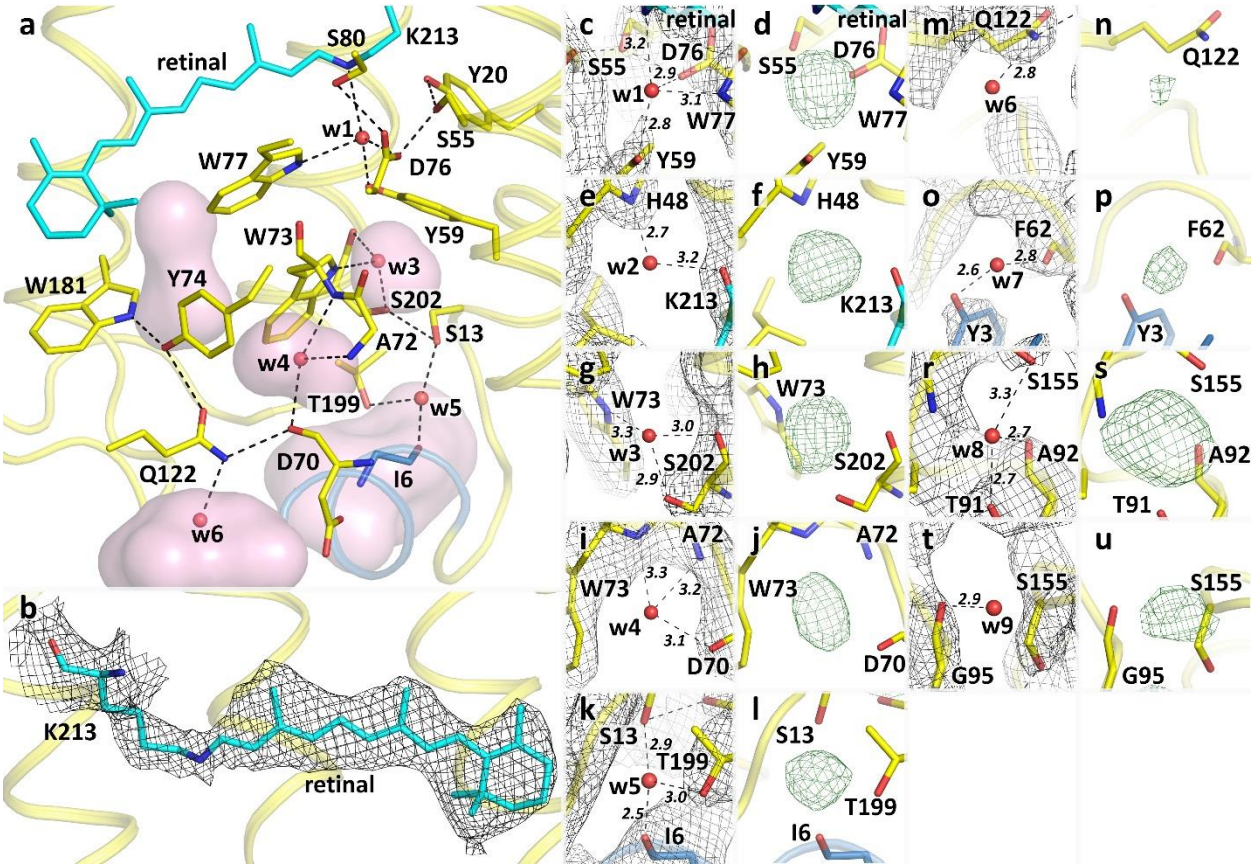

fig. S7. Details of the *Ns*XeR proton-translocation pathway. a. Key amino acids and protein active center. N-term helix is colored blue. **b.** Example of *Ns*XeR 2Fo-Fc electron density maps in the retinal region. The retinal is present in all-*trans* conformation and colored cyan. The maps are contoured at the level of 1.5σ. **c-u.** Example of *Ns*XeR 2Fo-Fc and Fo-Fc electron density maps near water molecules 1-9. The maps are contoured at the level of 1.5σ. Fo-Fc electron density maps are built with *Ns*XeR model missing water molecules. The Fo-Fc maps are contoured at the level of 3σ and colored green.

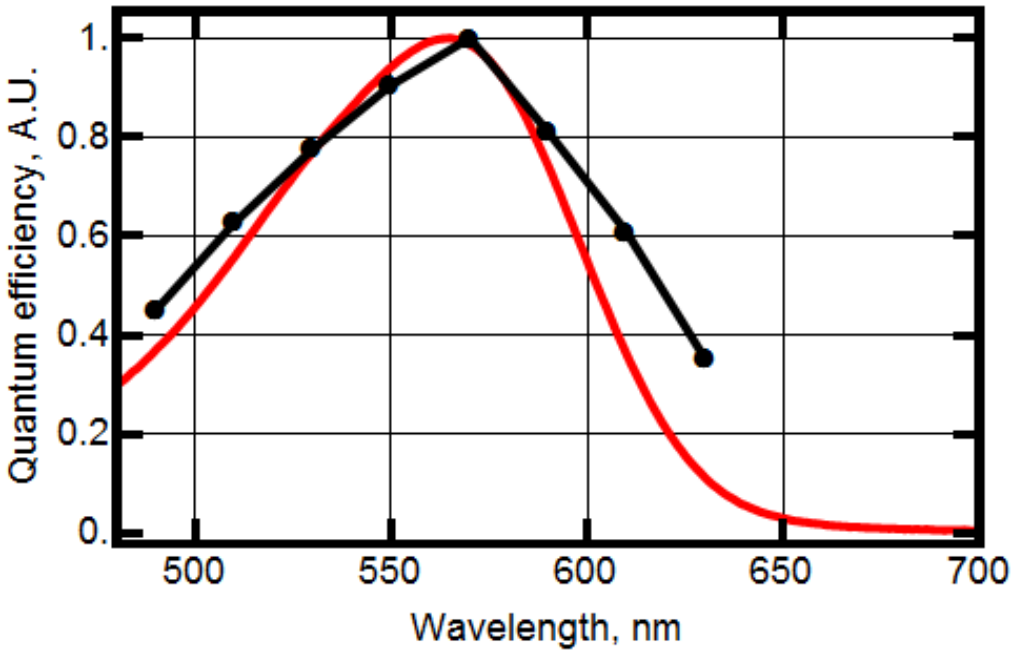

fig. S8. Action spectrum of photocurrents in NG108-15 cells expressing *Ns*XeR (black) and *Ns*XeR absorption spectrum (red).

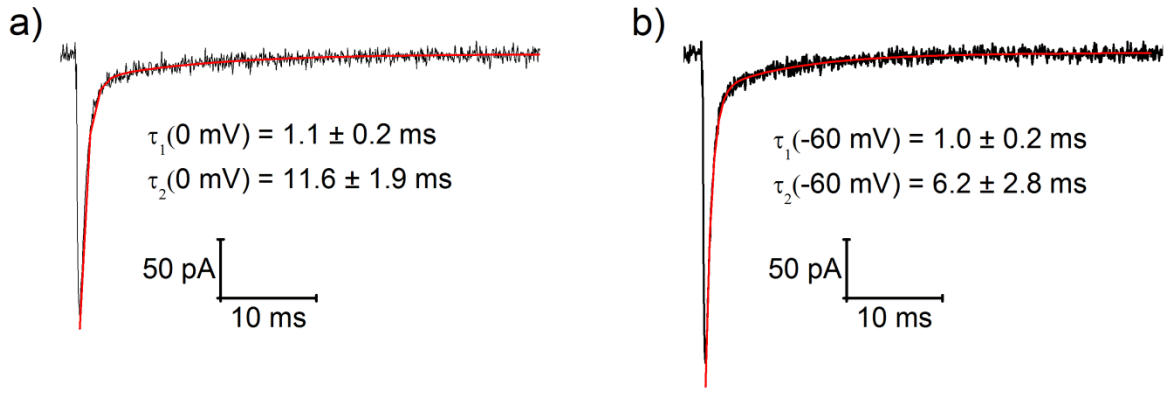

fig. S9. *Ns*XeR photocurrents in response to ultrashort light pulses. Nanosecond light pulses (λ = 560 nm) were generated by the Opolette 355 tunable laser system (OPTOPRIM). Shown are typical photocurrents which were measured in NG108-15 cells heterologously expressing *Ns*XeR at a membrane potential of a) 0 mV and b) -60 mV. The red line is a fit of the current decay using a biexponential function. Given are average τ_{off} values (n = 5) and the corresponding standard deviations.

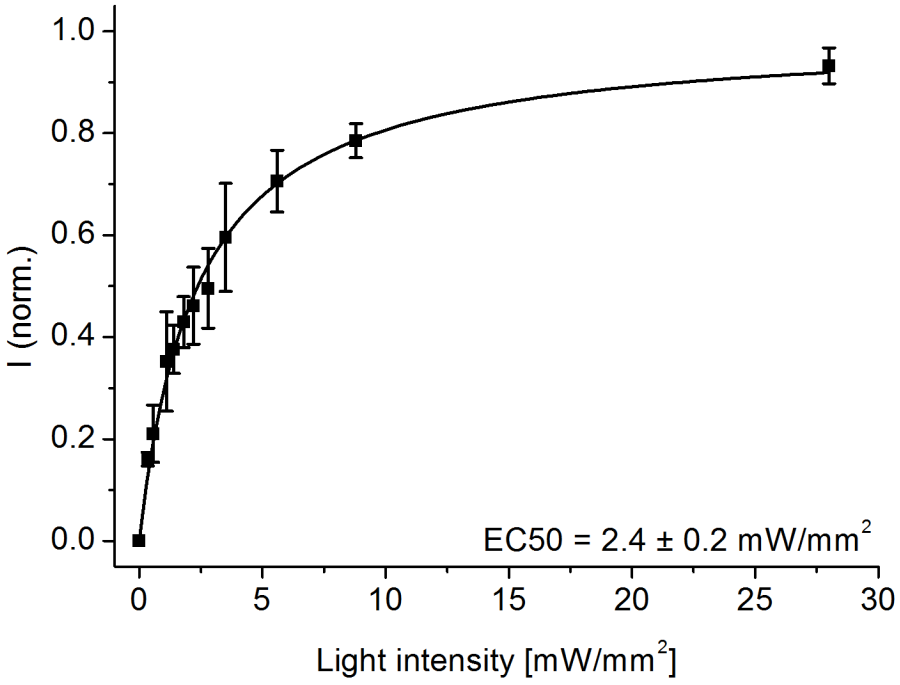

fig. S10. Light intensity dependence of *Ns*XeR. NG108-15 cells, heterologously expressing *Ns*XeR, C-terminally fused to the Kir2.1 membrane trafficking signal, were investigated by whole cell patch clamp experiments at a membrane potential of -100 mV. The photocurrents were measured in response to 500 ms light-pulses of indicated light intensities (λ=532 nm). The graphs show average values from normed stationary photocurrents (n=3) and the corresponding standard deviations. The solid line is a fit to the data using a hyperbolic model function with a half saturating value EC50 and a fixed v_{max}=1.

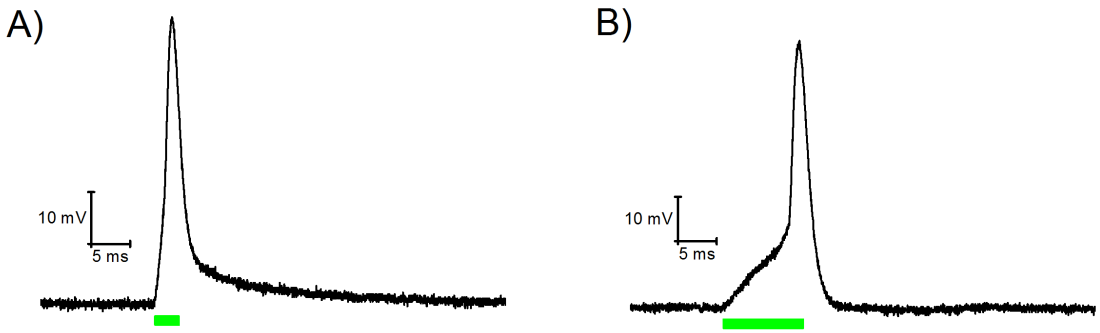

fig. S11. Variability of spike latency. Exemplary spiking traces measured in different neuronal cells. The light pulses had pulse widths of A) 3 ms and B) 10 ms. Rat hippocampal neurons heterologously expressing *Ns*XeR, C-terminally fused to the Kir2.1 membrane trafficking signal, were investigated by patch-clamp experiments in the whole cell configuration under current clamp conditions. The spikes were triggered by light pulses with a wavelength of $\lambda = 532$ nm and a saturating light intensity of 23 mW/mm^2. The current densities of the corresponding photocurrents, determined by measurements in the voltage clamp mode, were A) 15.3 pA/pF and B) 4.1 pA/pF.

table S1. Crystallographic data collection and refinement statistics.

Data collection	
Space group	$P2_12_12_1$
Cell dimensions	
a, *b*, *c* (Å)	64.01, 93.87, 196.21
α, β ,γ (°)	90, 90, 90
Resolution (Å)	50-2.5 (2.56-2.50)
R_{merge} (%)	28.6 (185.9)
$I / \sigma I$	9.56 (0.98)
Completeness (%)	100.0 (99.9)
CC (%)	99.9 (32.9)
Refinement	
Resolution (Å)	12-2.5
No. reflections	39282
R_{work}/R_{free} (%)	20.97/25.40
No. atoms	
Protein	5388
Water	54
Lipid fragments	545
Retinal	60
B factors (Å^2)	
Protein	38.2
Water	97.6
Lipid fragments	104.1
Retinal	34.6
r.m.s. deviations	
Bond lengths (Å)	0.0011
Bond angles (°)	0.4271

table S2. List of mutations to *Ns*XeR and their implications on proton pumping.

Proton translocation validation		
H48X		Not folded, cells not colored
D76E, D76N, D76S, D76T		Not folded, cells not colored
D220N	No pumping	Colored cells
D220E	Fully functional	
C212A, C212D		Not folded, cells not colored
C212S	Lowered pumping	
H94(ELRVG)	Lowered pumping	
Conservative aminoacids mutations		
W73R		Not folded, cells not colored
W73A	Strongly lowered pumping	Colored cells
W73Y	Lowered pumping	
S55A		Not folded, cells not colored
P209G	Strongly lowered pumping	
P209D		Not folded, cells not colored
N-terminus		
Δ2-12	Lowered pumping	Colored, not stable when solubilized
E4Q	Fully functional	
E4A, E4L	Lowered pumping	